EPJ manuscript No.
(will be inserted by the editor)

Symmetry breaking and clustering in a vibrated granular gas with several macroscopically connected compartments

J. Javier Brey[a], R. García-Rojo, F. Moreno, and M.J. Ruiz-Montero

Física Teórica. Facultad de Fisica. Universidad de Sevilla. Apartado de Correos 1065. 41080 Sevilla, Spain

Abstract. The spontaneous symmetry breaking in a vibro-fluidized low-density granular gas in three connected compartments is investigated. When the total number of particles in the system becomes large enough, particles distribute themselves unequally among the three compartments. Particles tend to concentrate in one of the compartments, the other two having the (relatively small) same average number of particles. A hydrodynamical model that accurately predicts the bifurcation diagram of the system is presented. The theory can be easily extended to the case of an arbitrary number of connected compartments.

1 Introduction

A granular system is an assembly of macroscopic particles or grains interacting inelastically, i.e. mechanical energy is not conserved. These systems exhibit many peculiar behaviors as compared with molecular, elastic systems [1]. One of them is the tendency to spontaneously segregate into high and low density regions, i.e. to form density clusters [2,3,4,5,6]. Therefore, they provide prime examples of formation of structures in far from equilibrium systems. The physical origin of this effect is the inelastic character of the interactions between particles. The simplest form of clustering is presented by freely evolving granular systems, as a consequence of a long-wavelength hydrodynamic instability [2,3,4]. However this is an ideal theoretical state that can not be generated experimentally.

Another interesting situation in which clustering effects show up, was observed several years ago in a seminal experiment [7]. A vertically vibrated system of grains was confined in a box separated into two equal connected parts by a wall of a certain height. For strong vibration, the particles distribute themselves on the average equally in the two compartments. Nevertheless, lowering the intensity of vibration (or the frequency) below a critical value, the spatial symmetry of the system is spontaneously broken, in the sense that a steady state is reached in which there is no equipartition of grains between the two compartments. Moreover, grains in the compartment with less number of particles have larger average kinetic energy than those in the high density part. By considering the exchange of particles between the two compartments as an effusion process, Eggers [8] proposed an analytical model to explain this phenomenon. Later on, the original experiment and also Egger's theory have been extended in different ways, considering systems with several compartments in which both clustering and declustering may occur [9], and also disperse mixtures of grains [10].

On the other hand, another symmetry breaking mechanism was reported in [11]. In this case, the equilibrium between the two compartments is hydrodynamic and not merely effusive. Consequently, this theory applies when the size of the opening connecting both sides is large as

[a] e-mail: brey@us.es

compared with the mean free path of the granular gas in its neighborhood. This is the opposite limit of that for which a balance of the flux of particles is enough to guarantee stationarity. The extension to binary mixtures of this hydrodynamic equilibrium has been investigated in [12], by means of molecular dynamics (MD). Let us also mention than while in Eggers' approach the external gravitations field plays an essential role, the mechanism put forward in ref. [11] is formulated in the zero gravitational field limit.

The aim of this contribution is to extend the study carried out in [11] to the case of several, more than two, connected compartments. The size of the holes connecting the compartments is considered 'macroscopic', i. e. larger than the mean free path of the granular fluid next to it.

It is a pleasure to dedicate this work to our good friend and colleague Carlos Pérez. We know he would have enjoyed discussing this kind of structure formation and had apportted interesting suggestions as well as key ideas for its better understanding.

2 The system and molecular dynamics simulation results

The granular fluid is often modeled as a system of N smooth inelastic hard spheres ($d = 3$) or disks ($d = 2$) of mass m and diameter σ. The inelasticity of the collisions is described by means of a constant, velocity independent, coefficient of normal restitution α, defined in the interval $0 < \alpha \leq 1$. This rather simplified model will be the one considered here. It has proven to qualitatively capture many of the experimental features of real granular systems. Then, when two particles i and j collide having pre-collisional velocities $\boldsymbol{v}_i$ and $\boldsymbol{v}_j$, respectively, their post-collisional velocities, $\boldsymbol{v}_i'$ and $\boldsymbol{v}_j'$, are given by

$$\boldsymbol{v}_i' = \boldsymbol{v}_i - \frac{1+\alpha}{2}(\widehat{\boldsymbol{\sigma}} \cdot \boldsymbol{v}_{ij})\widehat{\boldsymbol{\sigma}}, \tag{1}$$

$$\boldsymbol{v}_j' = \boldsymbol{v}_j + \frac{1+\alpha}{2}(\widehat{\boldsymbol{\sigma}} \cdot \boldsymbol{v}_{ij})\widehat{\boldsymbol{\sigma}}, \tag{2}$$

where $\boldsymbol{v}_{ij} \equiv \boldsymbol{v}_i - \boldsymbol{v}_j$ is the relative velocity before collision, and $\widehat{\boldsymbol{\sigma}}$ is the unit vector directed along the the line joining the centers of the two particles at contact, away from particle j.

The grains are enclosed in a box of width $3S$ and height L. For $d = 2$, S is a length, while for $d = 3$, it is an area. The box is divided into three equal compartments by two walls starting at a height h. A sketch of the system is given in Fig. 1. Collisions of particles with all the walls are elastic. To keep the system in a fluidized state, the wall located at the bottom is vibrated in a sawtooth way with a velocity v_b [13]. This means that all particles colliding with the wall find it moving 'upwards' with that velocity. Moreover, the amplitude of the vibration is considered much smaller than the mean free path of the gas in the vicinity of the wall, so the position of the wall can be taken as fixed. No external field acting on the particles is considered, something that can be understood as corresponding to the very strong shaking limit.

We have performed a series of MD simulations of the system described above in two dimensions, i.e. for a system of hard disks. In all cases, the simulations started with the same number of particles in each of the compartments and a Gaussian velocity distribution. For given values of α and v_b, a steady state is reached in which, on the average, the particles are equally divided into the three compartments, as long as its total number N is small. Nevertheless, when N is increased beyond a certain critical value, the spatial symmetry of the steady state is spontaneously broken. More specifically, in all the simulations we have carried out, it is observed that, after a transient period, the particles concentrate in one of the compartments, the other two having roughly the same much smaller number of particles. Moreover, particles in the high density compartment have significantly smaller velocity than particles in the low density ones. An example of a typical instantaneous snapshot is given in Fig. 2, which corresponds to a system of 500 inelastic hard disks with $\alpha = 0.9$. The height of the system is $L = 140\sigma$, and the width of each of the compartments $S = 100\sigma/3$. It is clearly seen that the number of particles in the central compartment is much larger than in the other two. The average density of the system is quite low. In particular, a dilute gas theory can be expected to apply in the lower part of the system, where there is no wall separating both compartments.

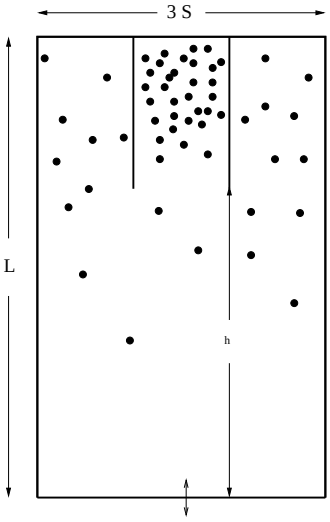

Fig. 1. Schematic picture of the set up considered. The wall at the bottom is vibrated in a sawtooth way with velocity v_b and small amplitude, while all the other walls are at rest. Collisions of the particles with all the walls are elastic

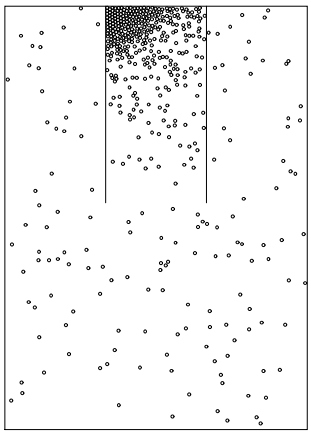

Fig. 2. Instantaneous snapshot of a typical configuration of a system in the steady state with broken spatial symmetry. The values of the parameters are $N = 500$, $\alpha = 0.9$, $L = 140\sigma$, $S = 100\sigma/3$, $h = 75\sigma$, and $v_b = 2\sqrt{\frac{2T(0)}{m}}$

To have a clearer idea of what actually happens in the system, the time evolution along a trajectory of the population of each of the compartments for the same system as considered in Fig. 2 is plotted in Fig. 3. Time has been scaled with the inverse of the initial Boltzmann collision frequency $\nu_0(0)$ given by

$$\nu_0(0) = \frac{2N\sigma}{3SL}\left(\frac{T(0)}{m}\right)^{1/2}, \tag{3}$$

where $T(0)$ is the (arbitrary) initial granular temperature of the particles. As usual, the granular temperature is defined from the average kinetic energy with the Boltzmann constant set equal to unity. It is observed that the symmetry of the system is broken very fast, and the system quickly evolves to a steady state in which the central compartment has about 400 particles, while the other other two compartments have about 50 each. It is worth to mention that in the

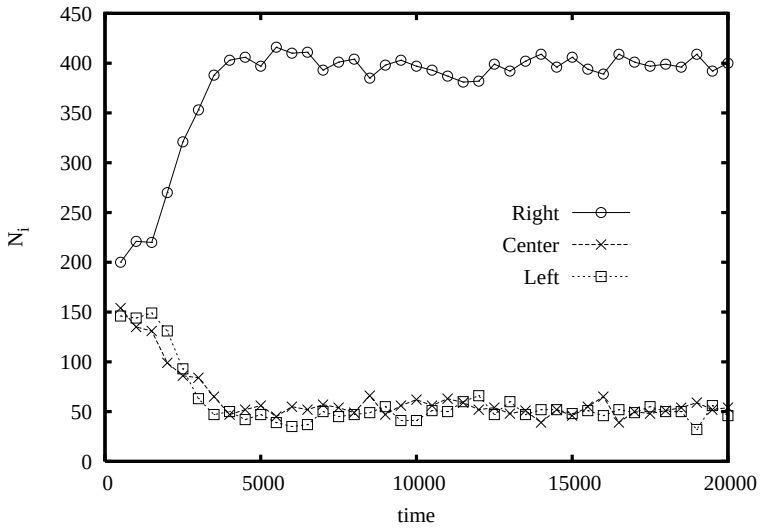

Fig. 3. Time evolution of the number of particles in each of the three compartments for the same system as considered in Fig. 2. Time is scaled with the inverse of the frequency given in Eq. (3)

figures shown here in relation with the time evolution of the system, only a relevant part of the latter is shown. The times reached in the simulations have always been much larger than those reported here in the figures, namely up to be really sure that the system was actually in a steady situation.

As already mentioned, in all the carried out simulations, it has been found that when the spatial symmetry is broken, the particles agglomerate in one of the compartments, the other two having approximately the same (low) number of particles. Nevertheless, in some cases in which the symmetry breaking proceeds rather slowly, the final state is reached after going through an intermediate time-dependent unstable state. For a given coefficient of restitution, this usually happens when the number of particles is high enough. In the intermediate state, two compartments have the same relatively large number of particles, while the number of particles in the third one is significantly lower. After some time, this configuration decays, and the number of particles in one of the populated compartments decreases until reaching the level of the other low density compartment. An example of this kind of behavior is provided in Fig. 4. The population of the central compartment grows for a while above the average, having the same value as that of the left compartment. Afterwards, the number of particles in it decreases until reaching the same value as in the right compartment.

The symmetry or asymmetry of the steady state can be characterized by the set of parameters

$$\epsilon_i \equiv \frac{\overline{N}_i}{N}, \tag{4}$$

with $\overline{N}_i$ being the average number of particles in the compartment i in the steady state. Of course, in a symmetric configuration, it is $\epsilon_i = 1/3$ for all i. The resulting bifurcation diagram is shown in Fig. 5, where the three parameters ϵ_i are plotted as a function of a dimensionless control parameter ξ_m, that is proportional to the total number of particles and will be defined below. The data for different values of α are seen to collapse on the same curves. Moreover, it has been found that the bifurcation diagram is not altered by modifying the velocity of the wall v_b, as long as it is large enough as to keep all the granular system fluidized. For small values of ξ_m, the three compartments are equally populated, but for $\xi_m > \xi_0$, one of the compartments has a larger number of particles than the other two. Note that the same symbol is used in the figure for the three compartments since they are equivalent, in the sense that they interchange their populations in different trajectories of the same system.

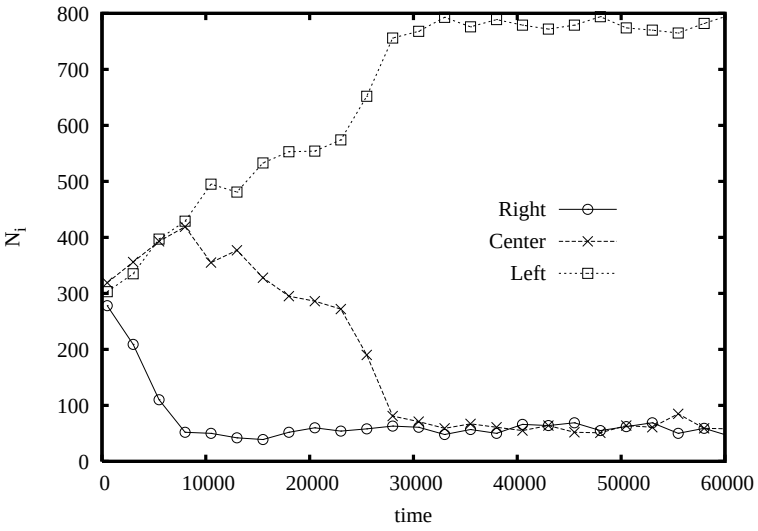

Fig. 4. Time evolution of the number of particles in each of the compartments for a system of $N = 900$ particles. The values of all the other parameters are the same as in Fig. 2. Note the slow relaxation of the system towards the steady state in this case as compared with that shown in Fig. 3

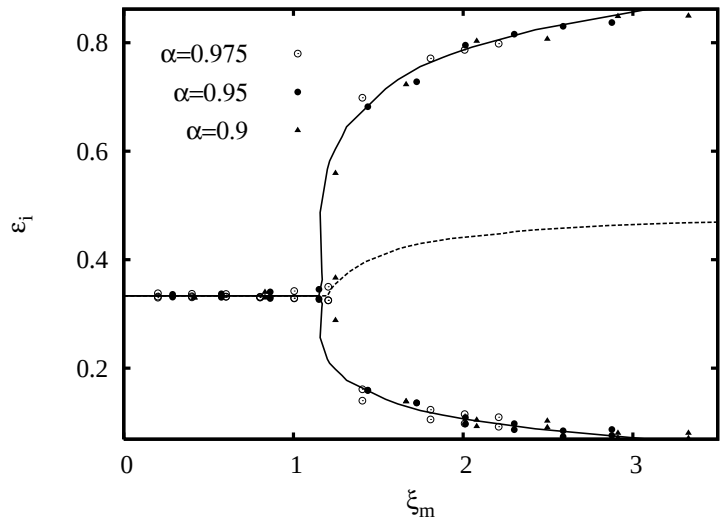

Fig. 5. Bifurcation diagram of the vibrated system with three compartments sketched in Fig. 1, showing the relative average number of particles in each compartment $\epsilon_i \equiv \overline{N}_i/N$, as a function of the dimensionless parameter ξ_m defined in the text. The symbols are MD results for the values of α indicated. The other parameters of the system are: $L = 140\sigma$, $S = 100\sigma/3$, and $v_b = 2\sqrt{2T(0)/m}$. The lines are the theoretical prediction from the model developed in the text, where its meaning is explained

3 The model

Consider the steady state reached by a vibrated dilute granular gas with only one compartment of width $3S$ and assume there are gradients only in the vertical direction, taken as the x axis. It is convenient to define a dimensionless space scale by

$$\xi = \sqrt{a(\alpha)} \int_0^x \frac{dx'}{\lambda(x')}\,, \tag{5}$$

where $\lambda(x)$ is the local mean free path given by

$$\lambda(x) = \left[C_d \sigma^{d-1} n(x)\right]^{-1}, \tag{6}$$

with $C_2 = 2\sqrt{2}$, $C_3 = \pi\sqrt{2}$, $n(x)$ the local number density, and

$$a(\alpha) = \frac{32(d-1)\pi^{d-1}\zeta^*(\alpha)}{(d+2)^3 C_d^2 \Gamma^2\left(d/2\right)\left[\kappa^*(\alpha) - \mu^*(\alpha)\right]}\,. \tag{7}$$

Here $\kappa^*(\alpha)$ and $\mu^*(\alpha)$ are the dimensionless transport coefficients characterizing the Navier-Stokes heat flux in a granular gas [14]. Finally, $\zeta^*(\alpha)$ is the dimensionless cooling rate due to the energy dissipation in collisions. The explicit expressions of these quantities can be found in ref. [15]. For elastic systems with $\alpha \to 1$, κ^* tends to unity, while μ^* and ζ^* vanish.

In the upper limit of the system $x = L$, ξ takes its maximum value $\xi_m \equiv \xi(x = L) = \sqrt{a(\alpha)} C_d \sigma^{d-1} N_x$, with $N_x \equiv N/3S$ being the number of particles per unit of section of the vibrating wall. This is the quantity used in the horizontal axis of Fig. 5. In the Navier-Stokes approximation, the hydrodynamic pressure of the system is uniform and can be expressed as [15]

$$p = \frac{T_0}{4 C_d \sigma^{d-1} L \sqrt{a(\alpha)}} f(\xi_m), \tag{8}$$

where T_0 is the temperature of the gas next to the vibrating wall and the function

$$f(\xi) \equiv \frac{2\xi + \sinh(2\xi)}{\cosh^2 \xi} \tag{9}$$

has been introduced. This function is plotted in Fig. 6. It presents a maximum at $\xi = \xi_0$, where $\xi_0 \simeq 1.20$ is the non-zero solution of the equation $\xi_0 \tanh \xi_0 = 1$. For large values of ξ it tends asymptotically to 2.

Now come back to the steady state reached by the system with the three compartments represented in Fig. 1. By extending the ideas developed in [11], we model this state by treating the compartments as independent, sharing only a thin, but macroscopic, layer of granular gas next to the vibrating wall at the temperature T_0. Macroscopic, hydrodynamic equilibrium between the three compartments requires that the pressure be the same in all them, and use of Eq. (8) gives

$$f(\xi_m^{(1)}) = f(\xi_m^{(2)}) = f(\xi_m^{(3)}), \tag{10}$$

where $\xi_m^{(i)}$ is the maximum value of ξ in the compartment i, i.e. next to the upper wall,

$$\xi_m^{(i)} \equiv \sqrt{a(\alpha)} C_d \sigma^{d-1} \frac{\overline{N}_i}{S}. \tag{11}$$

Since the total number of particles in the three compartments is N, the quantities $\xi_m^{(i)}$ must verify the condition

$$\xi_m^{(1)} + \xi_m^{(2)} + \xi_m^{(3)} = 3\xi_m = 3\sqrt{a(\alpha)} C_d \sigma^{d-1} N_x. \tag{12}$$

Of course, Eqs. (10) always have the symmetric solution $\xi_m^{(1)} = \xi_m^{(2)} = \xi_m^{(3)} = \xi_m$, in which the three compartments have the same average number of particles. From the observation of Fig. 6, it follows that this is the only solution for $\xi_m < \xi_0 \simeq 1.20$. On the other hand, for $\xi_m > \xi_0$ other solutions are possible since there are two different values ξ^- and ξ^+, $\xi^- < \xi^+$, for which $f(\xi^-) = f(\xi^+)$. Therefore, in this parameter region two asymmetric solutions are possible:

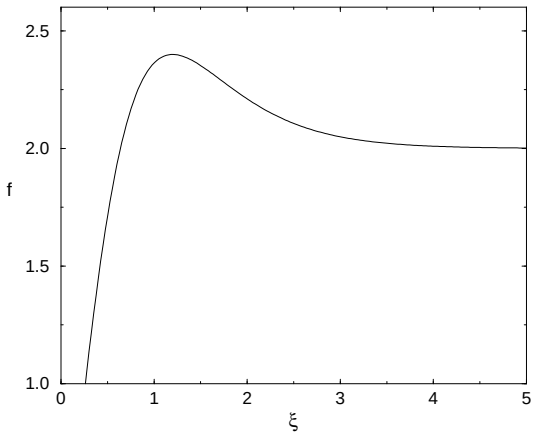

Fig. 6. The function $f(\xi)$ defined in Eq. (9). It characterizes the dependence of the pressure on the total number of particles in the one-compartment system

– *Asymmetric steady state I.* Two compartments have the same average number of particles, that is *smaller* than the average number of particles in the third one. Mathematically, it is defined by

$$2\xi_m^{-(I)} + \xi_m^{+(I)} = \xi_m. \tag{13}$$

– *Asymmetric steady state II.* Two compartments have the same average number of particles, that is *larger* than the average number of particles in the third one. It is defined by

$$\xi_m^{-(II)} + 2\xi_m^{+(II)} = \xi_m. \tag{14}$$

Given the value of $\xi_m > \xi_0$ characterizing the system under consideration, the two above asymmetric solutions are found by numerically solving the equation $f(\xi^-) = f(\xi^+)$ together with Eq. (13) or (14), respectively. This solutions are the lines plotted in Fig. 5. The upper (lower) solid line is the function $\xi_m^{+(I)}$ ($\xi_m^{+(II)}$). The dashed line is the function $\xi_m^{+(II)}$. The function $\xi_m^{-(II)}$ has not been plotted for the sake of clearness, taken into account that in the simulations, the system never was found in the asymmetric steady state II. Therefore, it seems that this state is unstable. It is seen that the agreement between the predicted values of the relative populations in the state II and the simulation results is pretty good. In particular, it is observed that their dependence on the coefficient of restitution α is scaled out when ξ_m is used as the control parameter.

The asymmetry of the stable state I increases very fast as the total number of particles in the system increases. Even more, it can be observed in the figure that the steady average number of particles in the two less populated compartments decreases as more particles are added to the system. Let us stress that, even when the number of particles in these compartments is rather small, the hydrodynamic description presented here describes quite accurately the asymmetry of the system.

4 Conclusions

It has been shown that the problem of the spontaneous symmetry breaking in a vibrated granular gas with three compartments connected by a macroscopic hole, can be treated in a way similar to the case of two compartments. In fact, the theory can be easily extended to deal with an arbitrary number of compartments. The only important point to be verified is that the hydrodynamic pressure and temperature near the vibrating wall are the same in all the compartments. In the simulations presented here, it was found that they agree within the

numerical precision of the measurements. Of course, the exhibited symmetry breaking becomes much richer as the number of compartments is increased.

An important point not yet well understood is why the system actually chooses the asymmetric state I with preference to the symmetric state and to the asymmetric state II, i.e. why the latter two are unstable. In principle, relevant information might be obtained by carrying out an stability analysis of the solutions. Nevertheless, such analysis is rather involved and has not been completed up to now. On the other hand, it is possible to compute the power dissipated in collisions for each of the states. This is done by taking into account that the energy balance requires that, in the steady state, the dissipated power be the same as the one injected through the vibrating wall. The latter for a system with a compartment is given by $v_b Sp$. For a system with three compartments, the powers dissipated in each of them have to be added up. Then, a simple analysis shows that it is maximum for the asymmetric state I. Also in the system with two compartments the asymmetric state dissipates more energy than the symmetric one.

It is worth to mention that some care is needed when studying the state discussed in this paper both by numerical simulations and also by experiments. The steady state of the system with one compartment discussed at the beginning of Sec. 3 is known to be unstable when its width is larger than a certain critical value. More precisely, the system experiments a continuos spontaneous symmetry breaking in the direction perpendicular to the heat flux, next to the wall opposite to the vibrating one [16,17]. The existence of this instability must be taken into account when deciding the sizes of the system to be used.

This research was supported by the Ministerio de Educación y Ciencía (Spain) through Grant No. FIS2005-01398 (partially financed by FEDER funds).

References

1. H.M. Jaeger, S.R. Nagel, and R.P. Behringer, Rev. Mod. Phys. **68** (1996) 1259-1273.
2. I. Goldhirsch and G. Zanetti, Phys. Rev. Lett. **70** (1993) 1619-1622.
3. I. Goldhirsch, M.L. Tan, and G. Zanetti, J. Sci. Comput. **8** (1993) 1-40.
4. S. McNamara and W.R. Young, Phys. Rev. E **50** (1994) R28-R34; **53** (1996) 5089-5100.
5. W. Losert, D.G.W. Cooper, and J.P. Gollub, Phys. Rev. E **59** (1999) 5855-5861.
6. J.S. Olafsen and J.S. Urbach, Phys. Rev. Lett. **81** (1998) 4369-4372 ; Phys. Rev. E **60**, (1999) R2468-R2471.
7. H.J. Schlichting and V. Nordmeier, Math. Naturwiss. Unterr. **49** (1996) 323-332.
8. J. Eggers, Phys. Rev. Lett. **83** (1999) 5322.
9. D. van der Meer, K. van der Weele, and D. Lohse, Phys. Rev. Lett. **88** (2002) 174302-1-4.
10. R. Mikkelsen, D. van der Meer, K. van der Weele, and D. Lohse, Phys. Rev. Lett. **89** (2002) 214301-1-4.
11. J.J. Brey, F. Moreno, R. García-Rojo, and M.J. Ruiz-Montero, Phys. Rev. E **65** (2001) 011305-1-4.
12. A. Barrat and E. Trizac, Mol. Phys. **101** (2003) 1713-1719.
13. S. McNamara and J-L. Barrat, Phys. Rev. E **55**, (1997) 7767-7770 ; S. McNamara and S. Luding, Phys. Rev. E **58** (1998) 813-822.
14. J.J. Brey, J.W. Dufty, C.S. Kim, and A. Santos, Phys. Rev E **58** (1998) 4638-4653.
15. J.J. Brey, M.J. Ruiz-Montero, and F. Moreno, Phys. Rev. E **62** (2000) 5339-5346.
16. E. Livne, B. Meerson, and P.V. Sasorov, Phys. Rev. E **65** (2002) 021302-1-6.
17. J.J. Brey, M.J. Ruiz-Montero, F. Moreno, and R. García-Rojo, Phys. Rev. E **65** (2002) 061302-1-10.